Mechanistic aspects of selected Phytochemicals against Severe Acute Respiratory Syndrome – Coronavirus 2: A molecular docking approach

Manikandaselvi. S,

PG and Research Department of Biochemistry,SengamalaThayaar Educational Trust Women's College (Autonomous),Sundarakkottai, Mannargudi, Thiruvarur DT, Tamilnadu, India.

ABSTRACT

Background: This globe is now seeing a pandemic epidemic of 'COVID-19′ produced by an RNA virus 'SARS-CoV-2'. Millions have died as a result of the sickness, and the number is growing by the day. The viral genome infects the human host via contact with the spike protein (S) and host GRP78, TMPRSS22. Most of the recently introduced vaccines across geographies, commonly target S. A recent increase in single/multiple mutations in the S region is cause for worry since it may evade vaccine-induced immunity. So far, the repurposed medicine therapy regimen has not proven very successful.

Hypothesis: Natural compounds have the ability to suppress SARS-CoV-2 by targeting both host and viral proteins.

Materials and methods: A hypothetical spike protein, human host proteins are docked with four phytochemicals such as Andrographolide, Caffeicacid, Piperine, Scutellareinand standard antiviral drug such as Remdesivir. Protein- Protein, Protein-Ligandsare docked.

Result: The findings of molecular docking revealed that phytochemicals of natural origin, have chosen four compounds, which have been suggested as SARS-CoV-2 inhibitors on the basis of the energy types of interaction of ligands with human receptors and ligands with spike protein.

Conclusion: This finding sheds light on the role of phytochemicals in preventing viral entrance and counteracting COVID-19 effects by limiting the interaction of S protein with human receptors, thus opening the door for COVID-19 therapy until a better choice becomes available.

Keywords: Molecular docking, SARS-CoV-2, Spike protein, Phytochemicals

INTRODUCTION

The Corona Virus Disease 2019 (COVID-19) infection, brought about by Severe Acute Respiratory Syndrome Coronavirus - 2 (SARS-CoV-2), emerged as a global pandemic and continues to raise grave concerns. As a direct result of the effective introduction of new vaccinations and the development of worldwide treatment methodologies, the

initial perplexity and apprehension surrounding this pandemic have subsided. The duration of this infection appears incalculable and speculative. Hence, researchers continue to seek for effectual treatments for acute infections, whether in immunocompromised individuals or if potentially lethal, vaccine-resistant new virus strains arise (Jeon et al., 2022). In order to keep infections at bay, apart from existing treatment methodologies, it's important to practice strategies that assist with management of symptoms in the long-term and also boost the immune system. From 3 January 2020 to 3 May 2023, WHO reported 44,952,996 confirmed cases of COVID-19 in India, with 531,564 fatalities. A total of 2,206,624,273 vaccine doses have been administered as of 10 April 2023 (https://covid19.who.int/region/searo/country/in). In this setting, and depending on the quality of medical care available in each nation, herbal medicines may be a viable COVID-19 therapeutic alternative. Respiratory system dysfunction and perhaps multi-organ failure have been linked to SARS-CoV-2 infection. The ACE2 receptor has a broad distribution in the nasal and oral mucosal epithelial cells, onto which the SARS-CoV2 binds and spreads. As the virus advances to the lungs (the primary site of infection), it impairs the senses of taste and scent. The infection process concludes with endocytosis and the exploitation of the host cell's apparatus for genome replication, transcription, assembly, and viral escape. (Poduri et al., 2020) Multiple organ failure occurs as a consequence of SARS-CoV2 infection of neighbouring cells after viral egress and subsequent invasion of organ systems. The four structural proteins that make up SARS-CoV-2 are Spike (S), Envelope (E), Membrane (M), and Nucleocaspid (N). These proteins assist the coronavirus in recognising the target cell's receptor, fusing with the membrane receptor to cause infection, and expanding deeper into the host. SARS-CoV2 pathogenesis begins with viral entry, which is mediated by the infection's highly glycosylated spike protein (S protein). SARS-S engages ACE2 as the entry receptor (Li *et al.*, 2003) and employs the cellular serine protease TMPRSS2 for S protein priming. The spike protein's transition from a closed to an open conformation (before binding to ACE2) is facilitated by the chaperon proteins GRP78 or HSPA5 and TMPRSS2 (Hoffmann et al., 2020; Ibrahim et al., 2020). The translation of the gene for the corona virus's replicase is the next stage of the virus's life cycle. The replicase gene encodes two large ORFS, rep1a and rep1b, encoding two co-terminals of polyproteins, pp1a and pp1ab. The nsps 1–16 contain pp1a and pp1ab polyproteins. nsp11 becomes nsp12 following extension of pp1a into pp1b (Ziebuhr*et al*., 2000). The nsp12 is responsible for replication and transcription of the viral genome. After the RNA replication and sub genomic synthesis, the viral structural proteinsare encoded and incorporated into the endoplasmic reticulum (ER). Such proteins pass through the secretory pathway into the Endoplasmic Reticulum-Golgi Intermediate Compartment (Krijnse*et al.*, 1994). There, viral genomes encapsulated by the N protein bud forming mature virions in ERGIC membranes that contain viral structural proteins.The S protein is a crucial factor that helps to determine host range and cell vulnerability, as well as a noteworthy target of immune responses induced by infection and immunisation. Considering that the structural integrity and cleavage activation of S protein are vital components of viral invasion and pathogenesis, therapeutic strategies that target S protein may lead to the development of potent antiviral drugs. TMPRSS2, a cell-surface protein generated by epithelial cells of specific tissues, including those of the aerodigestive tract, has been identified as a crucial component of the SARS-CoV-2 infection process. The S1 subunit containing the receptor binding domain and the S2 subunit containing the viral fusion machinery combine to produce the inactive precursor of the spike protein. The S proteins contain two distinct protease cleavage

sites, one at the S1/S2 subunit interface and another in the S2 subunit. As demonstrated for SARS-CoV-2, receptor binding can then commence, followed by the S2' site cleavage, which is required for the fusion event to occur. As a preliminary step towards facilitating host-cell entry, the viral hemagglutinin protein binds to the ACE2 produced by respiratory epithelial cells. In a subsequent stage, hemagglutinin is divided to initiate the internalisation of the virus. This second phase requires proteases from the host cell, particularly TMPRSS2 (Mollica et al., 2020; Strope et al., 2020). Inhibition of TMPRSS2 activity is therefore a potential method for preventing viral infection. Although it has been demonstrated that camostat, nafamostat, and aerosolized aprotinin inhibit TMPRSS2 protease activity in several countries, they are licenced for unrelated purposes. Since April 6, 2020, at least one phase I-II clinical trial of camostat for COVID-19 has been accepting participants (ClinicalTrials.gov; NCT04321096). It is unknown if camostat inhibits other trypsin-like proteases besides TMPRSS2 and causes clinical damage (Wang et al., 2020). According to multiple investigations (Bian and Li, 2021), ACE-2 is the primary receptor for SARS-CoV-2. However, there is no correlation between the abundance of ACE-2 and the severity of clinical problems in hepatocytes, astrocytes, and pericytes in the central nervous system (Singh et al., 2020). As a result, researchers have identified various entry points for viruses. Several receptors, including GRP78, have been associated with the pathogenesis of other corona virus members (Vankadari and Wilce, 2020). Cell surface GRP78 (CS-GRP78) is a viral receptor that is overexpressed and present on the cell surface of virtually all cells during times of stress. GRP78 is an essential endoplasmic reticulum (ER) chaperone (ShahriariFelordi et al., 2021).Viral infections and other diseases, including those that induce rapid alterations in the cellular microenvironment, can cause ER stress (Shin et al., 2021).

GRP78 is an essential chaperone protein that regulates the folding of other cellular proteins. Healthy cells require a smaller amount of GRP78 to function ordinarily, whereas stressed cells need more GRP78 to survive. Under pathological conditions, GRP78 translocates from the endoplasmic reticulum (ER) to the cell surface, where it serves as a co-receptor for a variety of signalling molecules and viral entry. According to Shin et al. (2022), the risk factors for severe symptoms and outcomes in COVID-19 patients are of critical importance. As SARS-CoV2 entry into host cells is a prerequisite for viral infection, this intervention point is incredibly alluring. The phytochemicals were selected based on the survey results, and PubMed was used to confirm that they were among those commonly employed to treat viral respiratory infections. With spike protein, coronavirus main proteinase, and papain-like protease, it was anticipated that andrographolide and its derivative would possess strong binding affinities. For each complex, simulations of molecular dynamics were conducted, and findings suggested that both compounds had significant affinity for their target molecules (Khanal et al., 2021). A molecular docking analysis was carried out for 16 semisynthetic andrographolides (AGP) against 5 SARS-CoV-2 enzymes main protease (Mpro, PDB: 6LU7), papain-like protease (PLpro, PDB: 6WUU), spike glycoprotein (S, PDB: 6VXX), NSP15 endoribonuclease (NSP15, PDB: 6VWW), and RNA-dependent RNA polymerase (RdRp, PDB: 6M71). Compounds 12, 14, and 15 exhibited greater binding affinities for all of the examined enzymes compared to AGP. AGP-15 exhibited - 8.6 kcal/mol for NSP15; AGP-10, 13, and 15 exhibited - 8.7, - 8.9, and - 8.7 kcal/mol,

respectively, for S; and AGP-16 exhibited - 8.7 kcal/mol binding/docking score for Mpro (Veerasamy and Karunakaran, 2022). Using Molegro Virtual Docker 7, a library of 27 caffeic-acid derivatives was screened against 5 proteins of SARS-CoV-2 to determine the binding energies and interactions between compounds and SARS-CoV-2 proteins. Khainaoside C, 6-O-Caffeoylarbutin, khainaoside B, and vitexfolin A are potent modulators of COVID-19 with higher binding energies against COVID-19 Mpro, Nsp15, SARS-CoV-2 spike S2 subunit, spike open state, and spike closed state structure, respectively (Adem et al., 2020). Curcumin and piperine bind directly to the receptors binding domain of S-protein and ACE-2 receptors of the host cell, inhibiting virus entrance into the host cell (Kumar et al., 2021). (Rasool et al., 2020) Saikosaponins (triterpene glycosides), Amentoflavone, Scutellarein, Myricetin, extracts of Isatisindigotica, and Houttuynia cordata are effective against 2019-nCoV. Myricetin, scutellarein, and phenolic compounds from Torreya nucifera and Isatisindigotica have been identified as natural inhibitors of SARS-CoV enzymes, including the nsP13 helicase and 3CL protease (Lin et al., 2005). Orientin is a natural flavonoid isolated from plants such as tulsi or holy basil, black bamboo, and passion flowers that can inhibit the interaction between the SARS-CoV-2 spike glycoprotein and its host receptor GRP78 (Bhowmik et al., 2021). Withanone and withaferin A found in Withaniasomnifera inhibit viral entry by targeting viral main protease and host TMPRSS2, and GRP78, respectively (Balkrishna et al., 2020). In addition, these phytochemicals were chosen through three fundamental steps: (1) The results of the survey were used to choose which ligands to use, and (2) PubMed was used to verify the use of those ligands in the treatment of viral respiratory infections. (3) Network pharmacology analysis for predicting all in vitro effects. As a result, we used a battery of bioinformatics techniques to assess how often these phytochemicals form complexes with receptors of human TMPRSS2, GRP78, and the SARS-CoV-2 spike protein. Predicted locations of molecular interactions between phytochemicals and receptors including TMPRSS2, GRP78, and SARS-CoV-2 spike protein are provided in addition to the structure-function link between phytochemicals and receptors.Therefore, along with other drugs currently tested against COVID-19, plant-based drugs should be included for speedy development of COVID-19 treatment. The current computational work focuses on identifying the dual role of phytochemicals on SARS-CoV-2 inhibition by targeting host and viral proteins.

Resources and Procedure

Software

Python Prescription 0.8 (PyRx) was utilised for optimising ligands and molecular docking, as it is incompatible with the AutoDock Vina module. The visualizer software of Discovery Studio is utilised for protein target preparation for docking and 2D visualisation of protein-ligand complexes following docking. This study utilised online resources such as Marvin JS chemaxon, SWISS MODEL, HADDOCK, RCSB PDB, NCBI, PubChem, ZINC, SWISSADME, and Molinspiration.

Phytochemicals Chosen

Selected phytochemicals include (Andrographolide (PubChem ID-5318517), Caffeicacid (PubChem ID-689043), Piperine (PubChem ID-638024), and Scutellarein (PubChem ID-5281697), as well as the antiviral drug Remdesivir (PubChem ID-121304016). The three-dimensional (3D) structures of these phytochemicals were obtained from the PubChem server (https://pubchem.ncbi.nih.gov/compound) in simple data format (sdf). Marvin JS chemaxon software was used to convert all ligands into pdb type, and they were optimised using Open babel in PyRx (version 0.8), which converted the ligands energetically to the most stable structures using Merck. To systematically evaluate the reactivity of the resulting plant-based bioactive compounds, Remdesivir and other standard pharmaceuticals were considered as controls.

phytochemical screening for pharmacological similarity

All ligands were evaluated based on Lipinski's rule of five parameters (molecular weight 500 Da, no more than 5 hydrogen bond donors, no more than 10 hydrogen bond acceptors, and AlogP 5) to determine their potential as drugs. The SWISSADME server was used to retrieve the Lipinski's rule of five parameters. This was accomplished by uploading the SMILES of the respective compounds to the web server and software.

Selected proteins for analysis

Crystal structures of the SARS-CoV-2 spike protein (PDB ID: 6VSB), TMPRSS2 receptor protein (PDB ID: 1Z8G), and GRP78 receptor protein (PDB ID: 5E84) were determined for this study. The receptors' 3D crystal structures were obtained from the Protein Data Bank (PDB) (www.pdb.org/pdb).

Docking Protein–Protein Interaction at the Molecular Level

The Easy interface of the HADDOCK 2.2 web-server was used to execute knowledge-based protein-protein coupling of the Spike protein with the human TMPRSS2, GRP78 receptor (Van Zundert et al., 2016). HADDOCK (https://wenmr.science.uu.nl) uses experimental data to guide the molecular docking process, as opposed to ab initio docking protocols that consider only the structures' coordinates (van Dijk et al., 2005). HADDOCK's docking strategy consists of three steps: 1) randomization of orientations followed by energy reduction to prevent steric conflicts, 2) torsion angle dynamics using torsion angles as degrees of freedom, and 3) refinement in Cartesian space with an explicit solvent. Before submitting the docking task, "active" residues were defined as those within the protein's ligand-binding pocket, while "passive" residues were automatically identified as those surrounding the active residues. The retrieval of ten clusters as HADDOCK results.

Interaction Protein–Ligand

The molecular docking was carried out utilising a flexible docking protocol, as described by Trott and Olson (2010), with minor modifications. For the molecular docking analysis of the selected phytochemicals with the target protein, Python

Prescription 0.8, a suite containing Auto Dock Vina, was utilised. The proteins' protein data bank, partial charge, and atom type (pdbqt) files were created. Except for the grid box, which was modified based on the active sites of each protein molecule, all bonds contained in phytochemicals were permitted to rotate freely, thereby rendering the receptor inflexible. After completing the molecular docking experiments and generating 10 configurations for each protein-ligand complex for all phytocompounds, text files of scoring results were also generated for manual comparison. The conformation with the lowest binding energy (kcal/mol) and root mean square deviation (rmsd) was deemed the optimal docking pose. For the duration of this investigation, an exhaustiveness of 10 was used for docking, and the number of modes was set to 10 in order to obtain more precise and reliable results. DSV was then used to prepare, visualise, and analyse the relationship between ligands and proteins.

RESULTS AND DISCUSSION

SWISS ADME and Molinspiration Explorer were used to predict druglikeness using Lipinski's criteria. Lipinski's rule of five indicates that a molecule is drug-like if it has a molecular weight less than 500 dalton, less than five H-bond donors, fewer than ten H-bond acceptors, and a LogP less than five (Lipinski, 2004).The results are presented in Table 1. All selected phytochemicals except standard drug showed good druglikeness properties.

Table 1: Lipinski's rule is used to predict druglikeness.

	Molecular weight (< 500)	AlogP (< 5)	H-Bond acceptor (< 10)	H-Bond donor (< 5)	Violations
Andrographolide (AND)	356	1.05	5	3	0
Caffeic acid (CAF)	180.16	0.94	4	3	0
Piperine (PIP)	285.34	3.33	4	0	0
Scutellarein (SCU)	286.24	2.20	6	4	0
Remdesivir	602.38	3.46	12	4	No; 2 violations: MW>500, NorO>10

Molecular Docking study on Spike protein with human receptors

S protein facilitates viral-cellular membrane fusion by binding to several surface structural and nonstructural receptors on host cells through its receptor-binding domain (RBD). The virus's spike protein is made up of two functional subunits: S1 and S2. The first, composed of four domains (S1 A, S1 B, S1 C, and S1 D), aids in the virus's attachment to the host cell receptor. The union of the two membranes is then coordinated by S2. This fusion stimulates proteases, allowing the S protein to be proteolytically cleaved. The latter triggers conformational changes in the S2 subunit, preparing it for viral-cell membrane fusion. Thus, RBD is the essential component that

allows the virus to enter cells through its communications with ACE2 and GRP78. Once within the host cell, the virus releases its RNA into the cytoplasm, which triggers the translation of its replicase gene. ORF1a/1b are two overlapping open reading frames inside the viral replicase gene. The ORFs are translated into polyproteins 1a and 1ab. The two polyproteins are then broken by two cysteine proteinases, the primary protease or 3-chymotrypsin-like protease (Mpro/3CLpro) and papain-like protease (PLpro), resulting in the release of 16 non-structural proteins (nsp1 to 16). The papain-like protease (nsp3), major protease (nsp5), RNA-dependent RNA polymerase (RdRp/nsp12), helicase (nsp13), and nsp15 (NendoU) have all been identified as potential antiviral therapeutic targets. Small compounds having the ability to influence the binding effectiveness of spike protein to its receptor may operate as a viral attachment inhibitor in both infections. To treat SARS-CoV-2 illness, many possible treatment techniques have been tested, including protein-based vaccine design, inhibition of human receptors, and the influence of phytochemicals on spike protein interaction with its human receptors. Among the several therapeutic options suggested for the treatment of SARS-CoV 2, medication creation using phytochemicals is a widely recognisedstrategy.

Molecular Docking study of Spike protein with GRP78

GRP78 is found in the lumen of the Endoplasmic Reticulum (ER) attached to and deactivating three enzymes responsible for cell death / differentiation (Activating Transcription Factor 6 (ATF6), Protein Kinase RNA-like Endoplasmic Reticulum Kinase (PERK), and Inositol-requiring Enzyme 1 (IRE1). GRP78 activates ATF6, PERK, and IRE1 when they reach a certain threshold of unfolded proteins. The activation of enzymes results in the inhibition of protein production and the promotion of refolding (Shen et al., 2002). GRP78 overexpression is also triggered by cell stress, increasing the likelihood that GRP78 will evade ER retention and relocate to the cell membrane. GRP78, once relocated to the cell membrane, is vulnerable to viral recognition through its substrate-binding domain (SBD) and may facilitate virus entry. The majority of previous studies assumed that ACE2 is the principal receptor of SARS-CoV-2. Providing GRP78 as a supplementary receptor in the presence of particular physiological circumstances where GRP78 expression is high (Ni et al., 2011) may make infection with SARS-CoV-2 more likely. Therefore, the existence of ACE2 and GRP78 in high concentrations may define these additional groups as extremely high-risk. It is thus critical to discover ways to prevent those who are at a higher risk of getting an aggressive type of SARS-CoV-2 infection. Human GRP78 receptor (PDB ID 5E84) is used in this work as a receptor protein for molecular docking of spike protein fragment (PDB ID 6VSB) with its receptor in human host. HADDOCK discovered eleven clusters that comprised 95.5% of the water-refined models. In terms of HADDOCK score (38.7 +/ 0.0) and Z-score (0.0), cluster one had the largest negative value. Van der Waals energy and electrostatic energy were shown to provide 33.2 +/ 4.5 kcal/mol and 303.7 +/ 21.7 kcal/mol, respectively. The BSA criteria was used to assess the quantity of protein surface that was not in contact with water. The structural

complex is compact, as evidenced by a higher BSA value of 1915.7 +/ 0.0. Furthermore, an RMSD of 32.2+/0.1 was recorded (Figure 1).

Figure 1 depicts Spike protein binding to the GRP78 receptor.

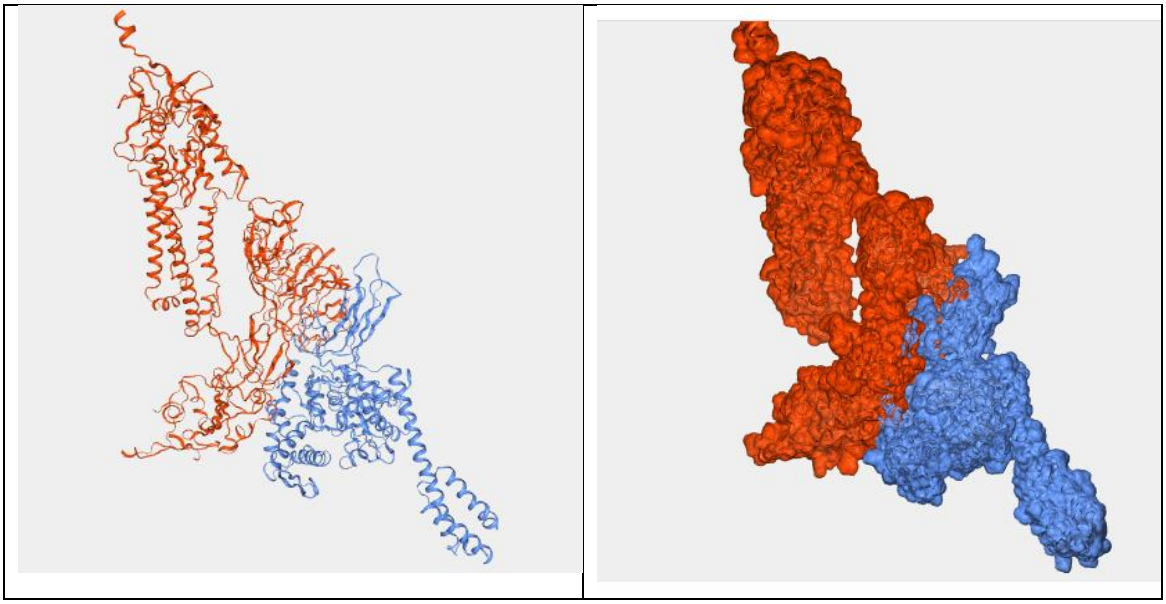

Molecular Docking study of Spike protein with TMPRSS2

According to recent research, both SARS-Corona Virus and SARS-Corona Virus-2 use the angiotensin-converting enzyme2 (ACE2) receptor for cell entry and Transmembrane protease serine type2 (TMPRSS2) to cleave the viral S glycoprotein, increasing viral activation, but SARS-CoV-2 transmits much more. Human TMPRSS2 receptor (PDB ID 1Z8G) is used in this work as a receptor protein for molecular docking of spike protein fragment (PDB ID 6VSB) to its receptor in human host. HADDOCK discovered eleven clusters that comprised 95.5% of the water-refined models. In terms of HADDOCK score (92.5 +/8.4) and Z-score (1.8), cluster one had the largest negative value. Van der Waals energy and electrostatic energy were shown to provide 52.5+/4.3 kcal/mol and 286.9 +/69.2 kcal/mol, respectively. The BSA criteria was used to assess the quantity of protein surface that was not coming into contact with water. The structural complex is compact, as evidenced by a higher BSA value of 2259.8 +/ 0.0. Furthermore, an RMSD of 13.6+/0.4 was recorded (Figure 2).

Figure 2 depicts Spike protein binding to the TMPRSS2 receptor.

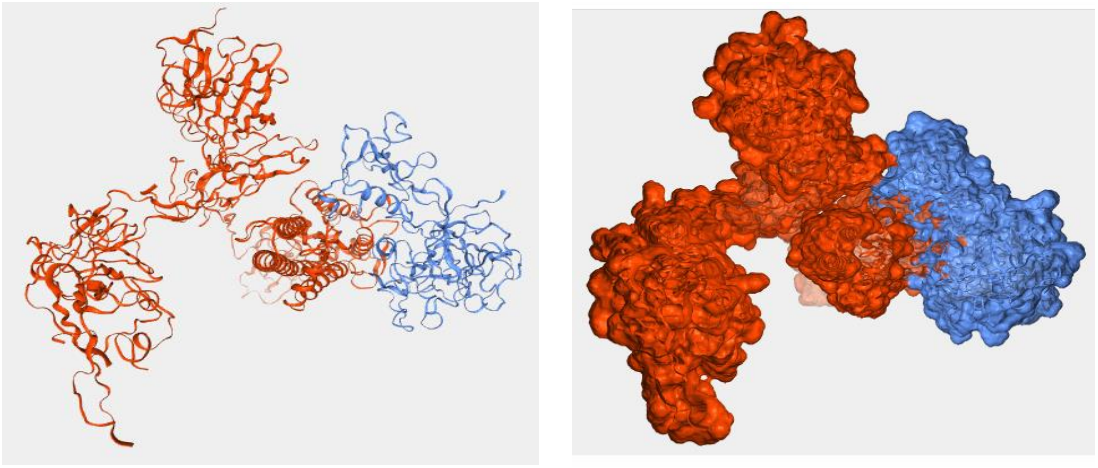

Protein-protein interaction data from molecular docking experiments suggested that the structural complex is compact.

Molecular Docking study on Spike protein (S) **and phytochemicals**

Table 3 shows the amino acids of S protein that interact with all of the identified ligands. The discovery studio visualise (DSV) was used to analyse the ligands' PyRx docking output '.pdbqt' files. DSV was used to create the 3D interaction, docking posture containing hydrogen bond donor surface, and 2D interaction picture of ligand docking on S protein. Figure 3 depicts the docking posture and interaction picture of chosen ligands with the greatest binding energy with S protein. AND, CAF, PIP, and SCU binding affinities at the interface of S protein were determined to be -8.5, -5.5, -6.8, and -7.2 kcal/mol, respectively (Table 2).

Table 2: Binding affinity of S protein and selected receptors protein with all selected phytochemicals

Ligand	Binding Affinity
postSpike-6vsb_B_Andrographolide5318517___uff_E=7846.11	-8.5
postSpike-6vsb_B_Caffeicacid689043_uff_E=57.94	-5.5
postSpike-6vsb_B_Piperine638024__uff_E=367.72	-6.8
postSpike-6vsb_B_scutellarein5281697__uff_E=179.24	-7.2
postSpike-6vsb_B_Remdesivir121304016_uff_E=5000.25	-9.2
postGRP785e84_Andrographolide5318517___uff_E=7846.11	-8.3
postGRP785e84_Caffeicacid689043_uff_E=57.94	-5.7
postGRP785e84_Piperine638024__uff_E=367.72	-7.5
postGRP785e84_scutellarein5281697__uff_E=179.24	-7.6
postGRP785e84_Remdesivir121304016_uff_E=5000.25	-8.9
postTMPRSS221z8g_Andrographolide5318517___uff_E=7846.11	-7.9
postTMPRSS221z8g_Caffeicacid689043_uff_E=57.94	-5.5
postTMPRSS221z8g_Piperine638024__uff_E=367.72	-7.3
postTMPRSS221z8g_scutellarein5281697__uff_E=179.24	-6.9
postTMPRSS221z8g_Remdesivir121304016_uff_E=5000.25	-9.4

Figure 3 shows the binding pocket of S proteinwith AND. AND binds with S proteinwith binding energy −8.5 kcal/mole. This docked structure is stabilized by one Hydrogen binding at LYS129 of S protein with O atom of AND, with bond length 5.77 Å and five alkyl binding at LUE141 (bond length 3.36 Å), VAL120 (2) (bond length 4.05, 4.36 Å), PHE157 (2) (bond length 4.63, 1.57Å) of S with AND.Figure 7 shows the binding pocket of S protein with CAF.S protein binds with CAF with binding energy –5.5 kcal/mole. This docked structure is stabilized by five H binding at THR827of bond length 2.62A^o, VAL952of bond length 2.77A^o, LEU945of bond length 2.04A^o, ASN953 (2) of bond length 1.71A^o, 1.71A^{o}and one Vanderwaal bonding at VAL826 with distance of 3.57A^{o}of S protein. The binding affinity of PIP at the interface of S protein was calculated as -6.8 kcal/mol. Figure 7 shows the binding pocket of S protein with PIP. This docked structure is stabilized by two pi-alkyl binding at VAL120 (2) at a distance of 3.72A^o, 4.41A^o and five hydrogen binding at VAL171 of bond length 4.46A^o, VAL127 of bond length 5.03A^o, VAL159 (2) of bond length 5.24A^o&4.31A^o, LEU141 of bond length 5.43A^o of S protein with PIP are noted.The binding affinity of SCU at the interface of S protein was calculated – 7.2kcal/mol. Figure 7 shows the binding pocket of S protein with SCU. Here, Spike protein binds with SCU with binding energy – 7.2 kcal/mole. This docked structure is stabilized by three H binding at SER373 of distance1.85A^o, at CYS336 of distance 2.66A^o, at ASP364A^o of distance 2.21 and also by two pi-alkyl at PHE338 of distance 5.05A^o, at PHE342 of distance 4.97A^o, two alkyl binding at VAL367 of distance 5.36A^o, 5.22A^{o}of spike protein with SCU is observed.

Figure 3shows the binding pocket of S protein with selected ligands

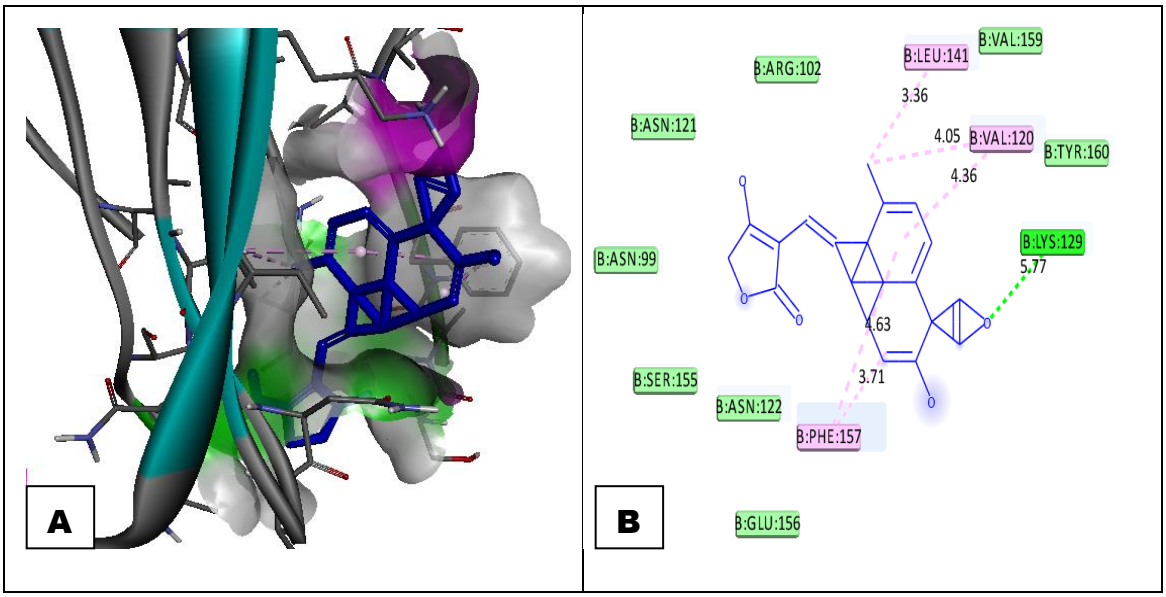

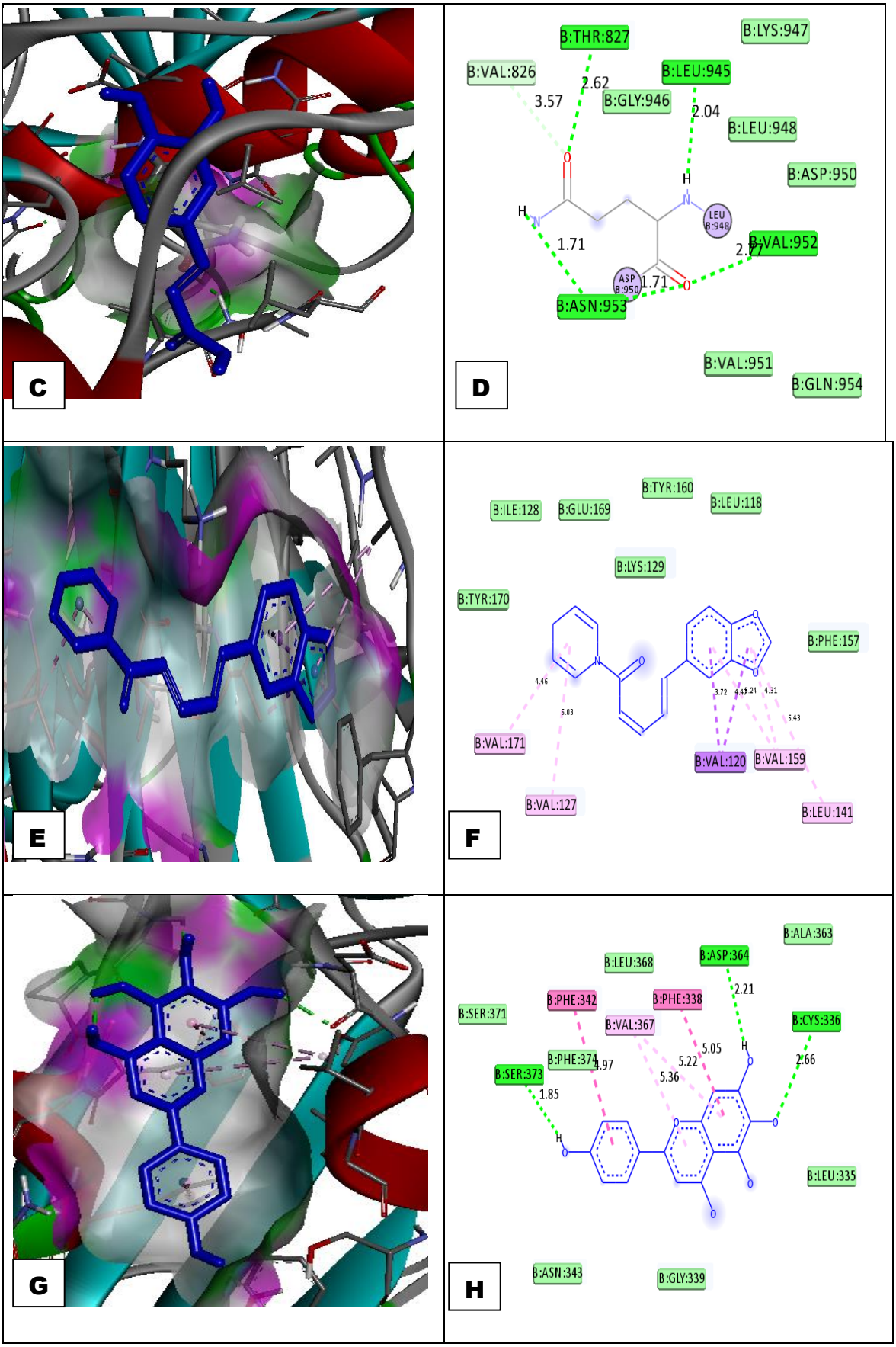
C
B:THR:827
B:LYS:947
B:VAL:826
B:LEU:945
2.62
3.57
B:GLY:946
2.04
B:LEU:948
B:ASP:950
LEU B:948
1.71
B:VAL:952
ASP B:950
1.71
B:ASN:953
D
B:VAL:951
B:GLN:954
E
B:TYR:160
B:ILE:128
B:GLU:169
B:LEU:118
B:LYS:129
B:TYR:170
B:PHE:157
4.46
5.03
3.72
4.45
4.24
4.31
5.43
B:VAL:171
B:VAL:120
B:VAL:159
B:VAL:127
B:LEU:141
F
G
B:ALA:363
B:LEU:368
B:ASP:364
2.21
B:PHE:342
B:PHE:338
B:SER:371
B:VAL:367
B:CYS:336
5.05
B:PHE:374
4.97
5.22
2.66
B:SER:373
5.36
1.85
B:LEU:335
H
B:ASN:343
B:GLY:339

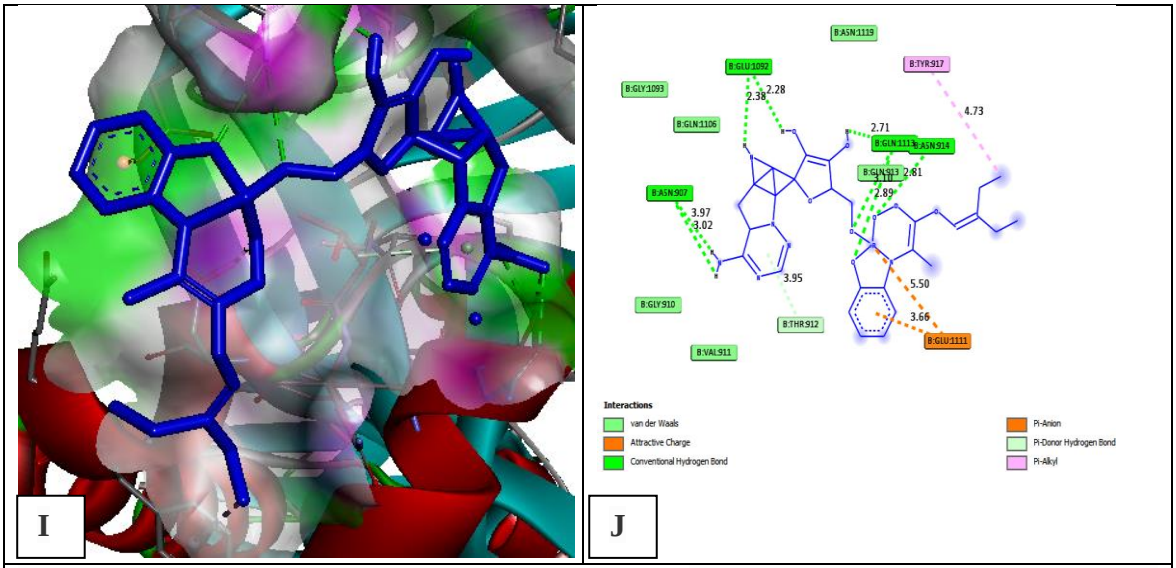

Docking with S. protein. **A** Docking pose of AND on hydrogen bonding surface. **B** 2D interaction of AND **C** Docking pose of CAF on hydrogen bonding surface. **D** 2D interaction of CAF. **E** Docking pose of PIP on hydrogen bonding surface. **F** 2D interaction of PIP. **G** Docking pose of SCU on hydrogen bonding surface. **H** 2D interaction of SCU.**I** Docking pose of Remdesivir on hydrogen bonding surface. **J** 2D interaction of Remdesivir.

GRP78 and phytochemicals were studied via molecular docking.

The binding affinity of AND,CAF, PIP and SCU at the interface of GRP78 was calculated as -8.3, -5.7, -7.5, -7.6 kcal/mol, respectively (Table 2). Table 3 shows the amino acids that interact with all of the chosen ligands for GRP78 proteins. The discovery studio visualise (DSV) was used to analyse the ligands' PyRx docking output '.pdbqt' files. DSV was used to create the 3D interaction, docking posture with hydrogen bond donor surface, and 2D interaction picture of ligand docking on GRP78 protein. Figure 4 shows the docking posture and interaction picture of chosen ligands with the greatest binding energy with GRP78. Figure 4 depicts GRP78's binding pocket with AND. AND has a binding energy of 8.3 kcal/mole with GRP78. This docked structure is stabilized by two Hydrogen binding at LYS344 of GRP78 protein with O atom of AND, with bond length 5.91 Å , at ARG101 with the distance of 2.00Å and two alkyl binding at LUE1422(2) (bond length 3.80, 4.51Å) of GRP78 with AND.Figure 4 shows the binding pocket of GRP78 protein with CAF.GRP78 protein binds with CAF with binding energy –5.7 kcal/mole. This docked structure is stabilized by five H binding at ASP38 of bond length 2.10A^o, at LYS96 of bond length 5.60A^o, at GLY227 of bond length 2.53A^o, at GLY228 of bond length 1.98A^o, at ALA229 with distance of 2.39A^o of GRP78 protein. The binding affinity of PIP at the interface of GRP78 protein was calculated as -7.5 kcal/mol. Figure 4shows the binding pocket of GRP78 protein with PIP. This docked structure is stabilized by four alkyl binding at PRO341(2) at a distance of 4.46A^o, 5.10A^o, at HIS473 of bond length 5.44A^o, at LEU422 of bond length 4.72A^o,one hydrogen binding at THR251 of bond length

2.38A^{o}and one vanderwaals binding at SER337 of bond length 3.46A^{o}of GRP78 protein with PIP are noted.The binding affinity of SCU at the interface of GRP78 protein was calculated – 7.6 kcal/mol.Figure 4shows the binding pocket of GRP78 protein with SCU. This docked structure is stabilized by one H binding at LYS296 of distance 2.48A^o, at ARG297 four different binding occur as one hydrogen binding of distance 2.44 A^o, one alkyl binding of distance 3.86, two pi-cation binding of distance 4.56 A^o, 4.78 A^o and at ARG367 one hydrogen binding of distance 2.73 A^o and one alkyl binding of distance 4.38 A^o occur. At GLY364 two pi-alkyl binding occur at the distance of 3.55 A^o, 4.26 A^o, at GLU293 pi-cation binding of distance 4.81 A^o, at SER365 unfavourabledonar-donar bond of GRP78 protein with SCU is observed.

Figure4 shows the binding pocket of GRP78 with selected ligands.

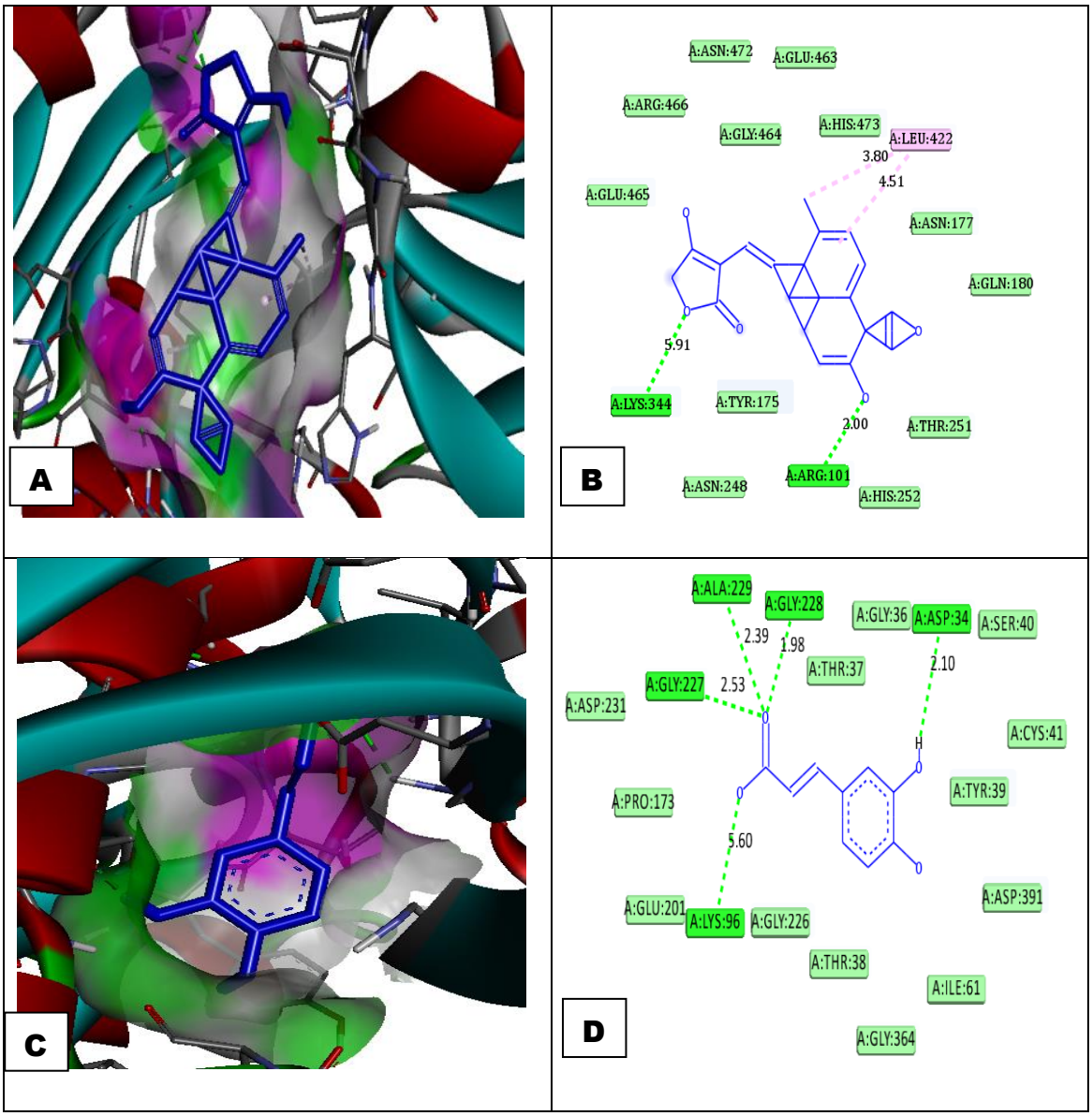

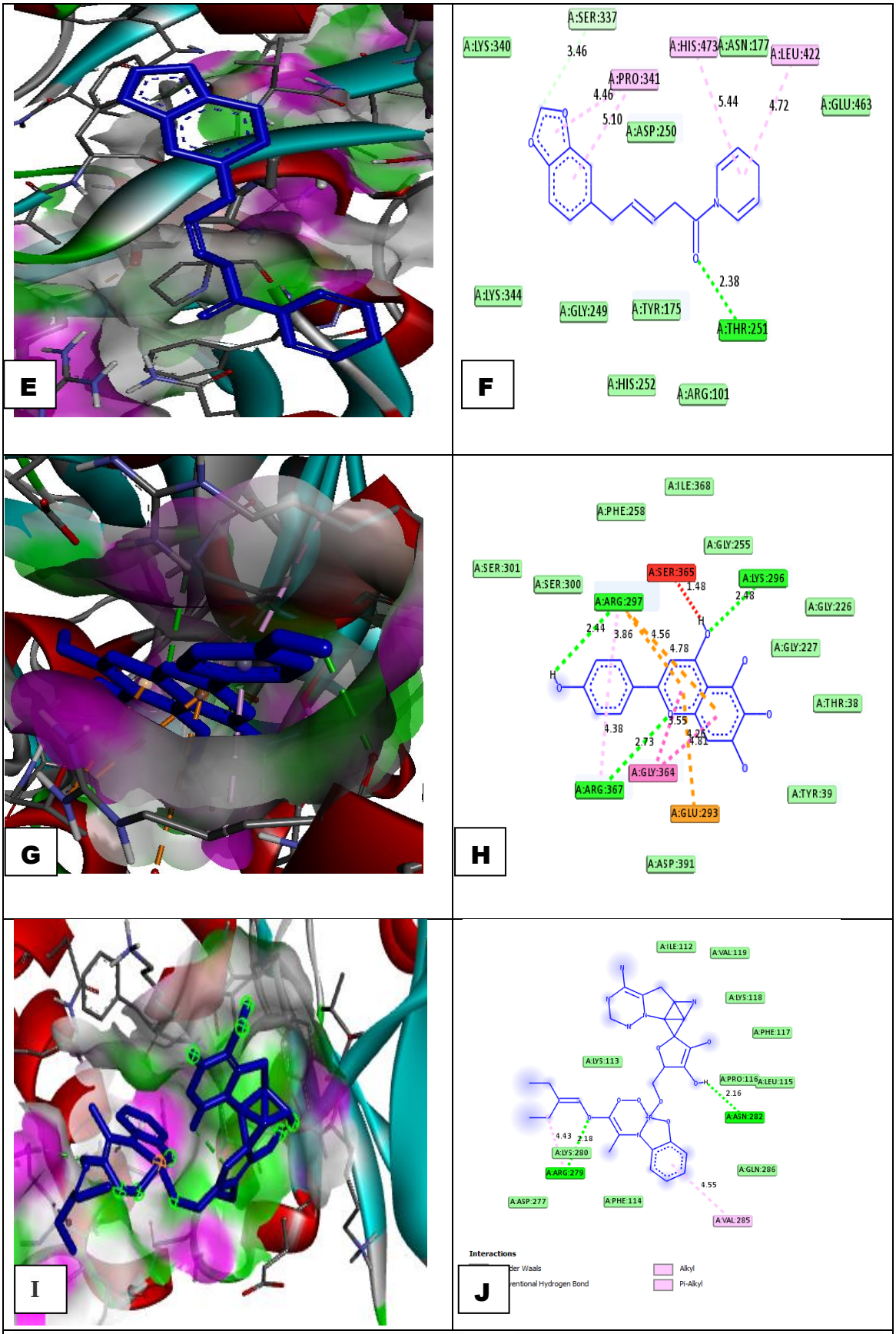

Docking with GRP78. A. Docking pose of AND on hydrogen bonding surface. **B** 2D interaction of AND **C** Docking pose of CAF on hydrogen bonding surface. **D** 2D interaction of CAF. **E** Docking pose of PIP on hydrogen bonding surface. **F** 2D

interaction of PIP. **G** Docking pose of SCU on hydrogen bonding surface. **H** 2D interaction of SCU. **I** Docking pose of Remdesivir on hydrogen bonding surface. **J** 2D interaction of Remdesivir.

TMPRSS2 and phytochemicals studied using molecular docking experiments

The binding affinity of AND,CAF, PIP and SCU at the interface of TMPRSS2 was calculated as -7.9, -5.5, -7.3, -6.9 kcal/mol, respectively (Table 2). Table 3 shows the interaction amino acids of TMPRSS2 proteins with each of the identified ligands. The discovery studio visualise (DSV) was used to analyse the ligands' PyRx docking output '.pdbqt' files. DSV was used to create the 3D interaction, docking posture with hydrogen bond donor surface, and 2D interaction picture of ligand docking on TMPRSS2 protein. Figure 5 depicts the docking posture and interaction picture of chosen ligands with the greatest binding energy to TMPRSS2. Figure 5shows the binding pocket of TMPRSS2 with AND. AND binds with TMPRSS2with binding energy −7.9 kcal/mole. This docked structure is stabilized by two Hydrogen binding at LEU132 of TMPRSS2 protein with O atom of AND, with bond length 1.88 Å , at LYS68 with the distance of 2.45Å,two alkyl binding at LEU132 with the distance of 4.09Å and at LYS68 with the distance of 5.25Å of TMPRSS2 with AND.Figure 5 shows the binding pocket of TMPRSS2 with CAF. CAF binds with TMPRSS2with binding energy −5.5kcal/mole. This docked structure is stabilized by three Hydrogen binding at TYR243, ARG210, ALA202 of TMPRSS2 protein with O atom of CAF, with bond length 2.70, 3.21, 2.32Å respectively, One alkyl binding at PRO245 with the distance of 5.43Å, onevanderwaalsbindng at PRO206with bond length 3.21Åand one unfavorable donar-donar interaction at PHE205 of TMPRSS2 with CAF.Figure 5shows the binding pocket of TMPRSS2 with PIP. PIP binds with TMPRSS2with binding energy −7.3kcal/mole. This docked structure is stabilized by three alkyl binding at LEU132, LYS68, PRO53 with the distance of 5.46, 5.24, 3.85Å of TMPRSS2 with PIP.Figure 5shows the binding pocket of TMPRSS2 with SCU. Here, LYS780 form one alkyl bond (length – 5.13A^o) with SCU. LYS780 of distance 2.30A^o, SER784 of distance 2.24A^o, ASP711 of distance 2.00A^o, HIS133 of distance 2.06A^o, PHE134 of distance 2.90A^{o}hydrogen bonding with SCU through is noted.

Figure5shows the binding pocket of TMPRSS2 with selected ligands.

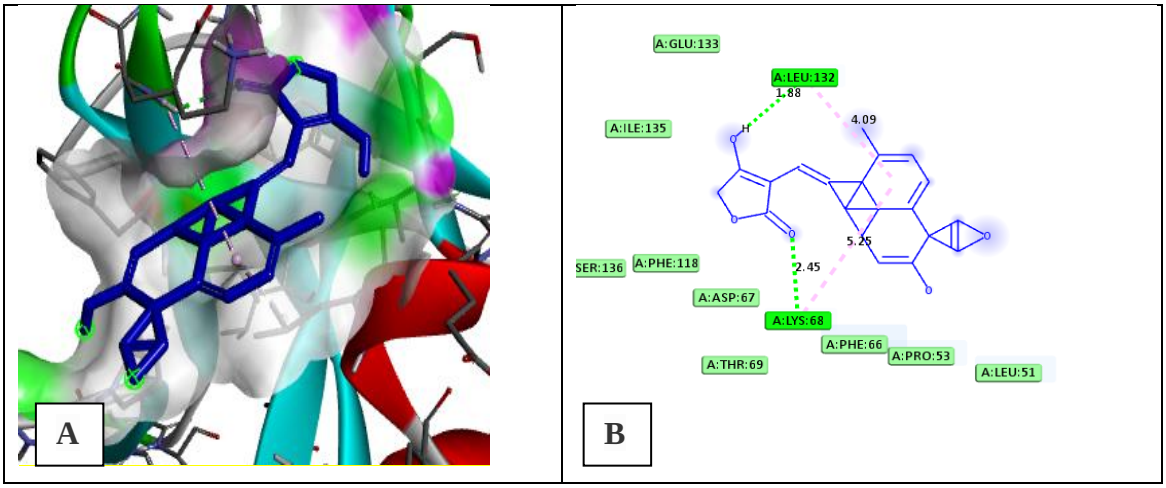

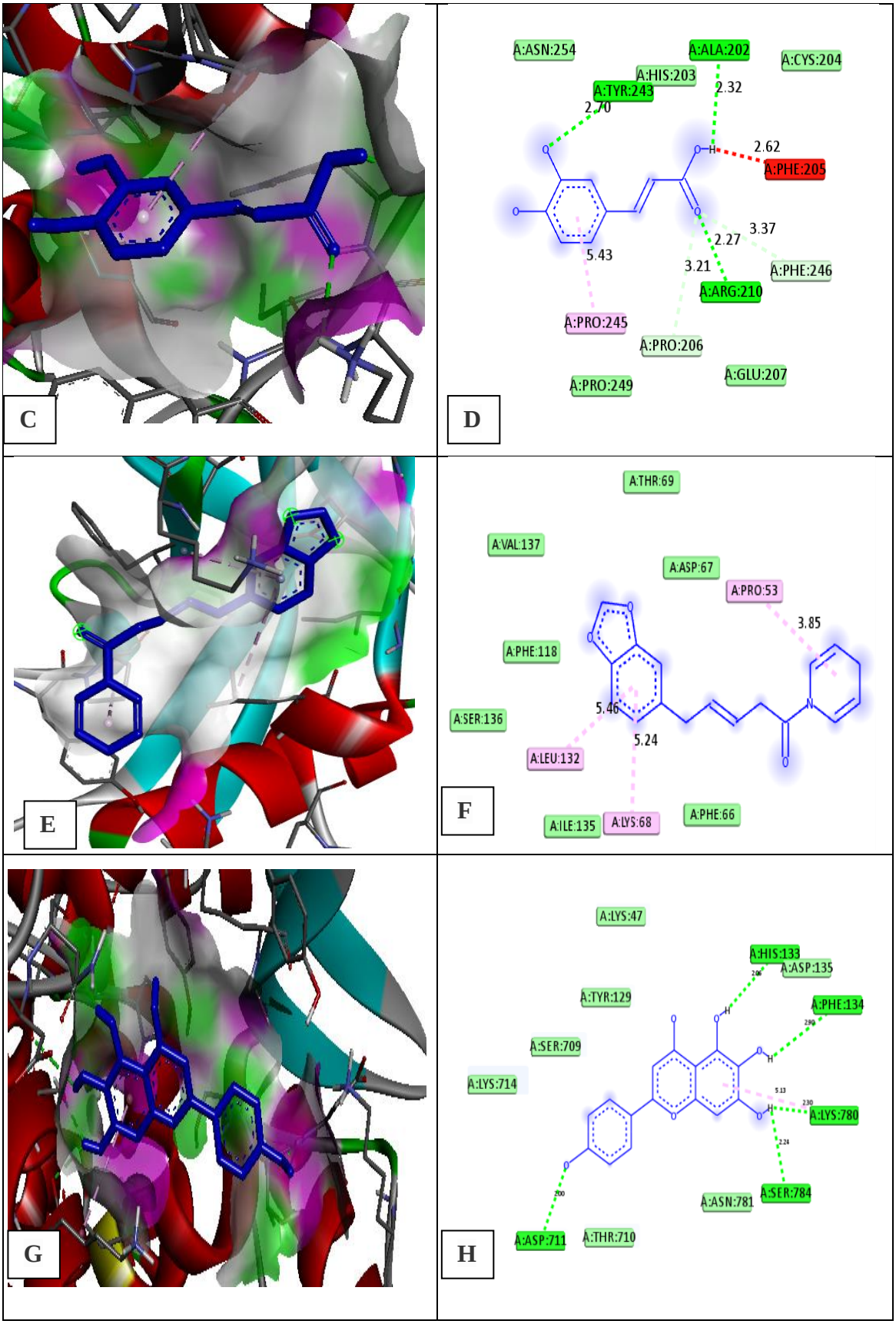
C
A:ASN:254
A:ALA:202
A:CYS:204
A:HIS:203
A:TYR:243
2.32
2.70
2.62
A:PHE:205
3.37
2.27
5.43
3.21
A:PHE:246
A:ARG:210
A:PRO:245
A:PRO:206
A:GLU:207
A:PRO:249
D
E
A:THR:69
A:VAL:137
A:ASP:67
A:PRO:53
3.85
A:PHE:118
5.46
A:SER:136
5.24
A:LEU:132
F
A:ILE:135
A:LYS:68
A:PHE:66
G
A:LYS:47
A:HIS:133
A:ASP:135
A:TYR:129
A:PHE:134
A:SER:709
A:LYS:714
A:LYS:780
A:ASN:781
A:SER:784
A:ASP:711
A:THR:710
H

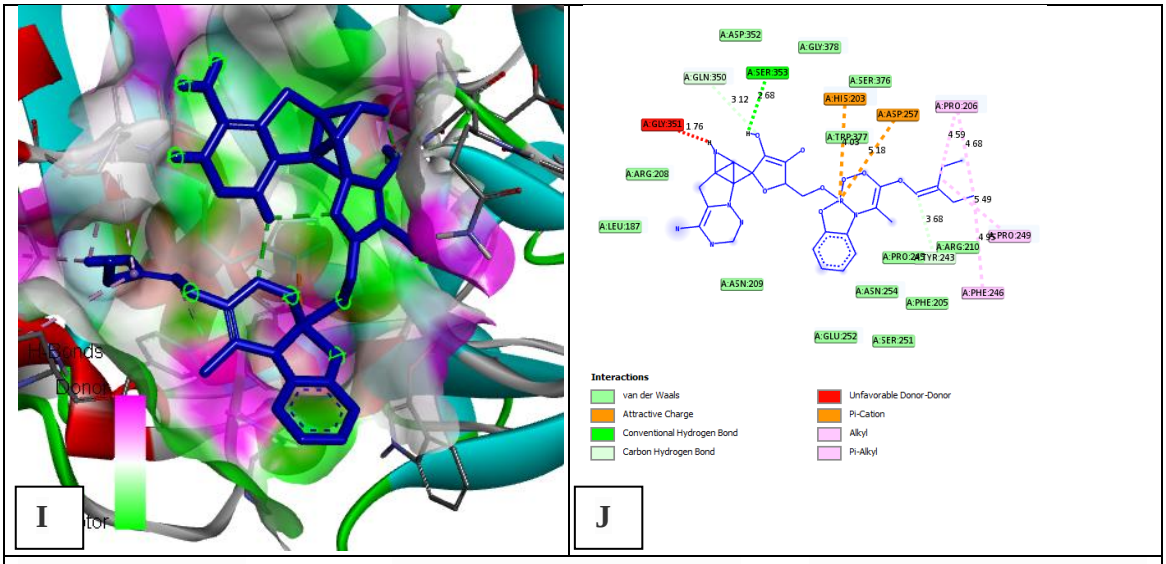

Docking with TMPRSS2 A. Docking pose of AND on hydrogen bonding surface. **B** 2D interaction of AND **C** Docking pose of CAF on hydrogen bonding surface. **D** 2D interaction of CAF. **E** Docking pose of PIP on hydrogen bonding surface. **F** 2D interaction of PIP. **G** Docking pose of SCU on hydrogen bonding surface. **H** 2D interaction of SCU. **I** Docking pose of Remdesivir on hydrogen bonding surface. **J** 2D interaction of Remdesivir.

Detailed analysis of intermolecular contacts of viral, human receptors and selected phytochemicals

Predicting binding affinity from structural models of viral, human receptors - phytochemicals interaction, plays an important role in drug design. Comparative study for viral, human receptors - phytochemical binding interaction energy values as obtained in our research work is shown in the following table 3.

Table 3Comparative study for ACE2 protein-ligand binding

Ligands	**S protein-ligand binding**	**GRP78protein-ligand binding**	TMPRSS2**protein-ligand binding**
AND	PHE157 (2), LEU141, VAL120 (2), LYS129	LYS344, ARG101, LEU(2)422	LEU132(2), LYS68(2)
CAF	THR827, VAL826, LEU945, VAL952, ASN953(2)	GLY227, ALA229, GLY228, ASP34, LYS96	TYR243, ARG210, ALA202, PRO245, PRO206, PHE205
PIP	VAL171, VAL127, VAL120 (2), VAL159 (2), LEU141	SER337, PRO(2)341, HIS473, LEU422, THR251	LEU132, LYS68, PRO53
SCU	ASP364, PHE338, CYS336, VAL367(2), PHE342, SER373	ARG(5)297, SER365, LYS296, ARG(2)367, GLY(2)364, GLU293	ASP711, SER784, LYS780(2), PHE134, HIS133

The phytochemicals with the greatest binding energy are thought to be the best inhibitors for the target molecule spike protein, which is generated by the interaction of a spike protein fragment with its human receptors. Following an in-silico mutagenesis investigation and experimental validation, human receptors p and phytochemicals such

as andrographolide, caffeic acid, piperine, and scutellarein may be employed for COVID-19 therapy.

CONCLUSION

Since it was hypothesised that inhibiting viral spike protein and/or human receptors might assist improve a medication or vaccine against Covid-9, the current investigation focused on small compounds that have the capacity to function against SARS-Cov-2 by disrupting the spike-human receptors connection. In this investigation, the phytochemicals andrographolide, caffeic acid, piperine, and scutellarein were employed. According to the docking investigation, the bioactives andrographolide, caffeic acid, piperine, and scutellarein had greater binding affinities with the human receptors. Consequently, the phytochemicals prevent spike protein from interacting with human receptors. This study revealed phytochemicals that could function as possible therapeutic agents against Covid-19; this goal necessitates hands-on investigations as well as in-vitro and in-vivo studies for clinical trialresearch.

CONFLICT OF INTEREST

The authors declare no conflict of interest

ACKNOWLEDGMENT

Authoris thankful to the Management of SengamalaThayaar Educational Trust Women's College (Autonomous), Mannargudi for providing financial support as seed money scheme and also provides all the necessary facilities related to the present research work.

REFERENCES

Abdelli I, Hassani F, BekkelBrikci S, and Ghalem S. *In silico* study the inhibition of angiotensin converting enzyme 2 receptor of COVID-19 by *Ammoidesverticillata* components harvested from Western Algeria. Journal of biomolecular structure & dynamics, 2021, *39*(9), 3263–3276. https://doi.org/10.1080/07391102.2020.1763199

Balkrishna A, Pokhrel S, Singh H, Joshi M, Mulay VP, Haldar S, Varshney A. Withanone from *Withaniasomnifera* Attenuates SARS-CoV-2 RBD and Host ACE2 Interactions to Rescue Spike Protein Induced Pathologies in Humanized Zebrafish Model. Drug Des DevelTher. 2021 Mar 11;15:1111-1133. doi: 10.2147/DDDT.S292805.

Bhowmik A, Biswas S, Hajra S, Saha P. *In silico* validation of potent phytochemical orientin as inhibitor of SARS-CoV-2 spike and host cell receptor GRP78 binding. Heliyon. 2021 Jan;7(1):e05923. doi: 10.1016/j.heliyon.2021.e05923.

Carlos AJ, Ha DP, Yeh DW, Van Krieken R, Tseng CC, Zhang P, Gill P, Machida K, Lee AS. The chaperone GRP78 is a host auxiliary factor for SARS-CoV-2 and

GRP78 depleting antibody blocks viral entry and infection. J Biol Chem. 2021 Jan-Jun;296:100759. doi: 10.1016/j.jbc.2021.100759.

Gorbalenya E, Enjuanes L, Ziebuhr J and Snijder EJ. Nidovirales: evolving the largest RNA virus genome, Virus Res., 2006, 117, 17-37, 10.1016/j.virusres.2006.01.017

Hebert-Schuster M., Rotta B. E., Kirkpatrick B., Guibourdenche J. and Cohen M. 2018 The interplay between glucose-regulated protein 78 (GRP78) and steroids in the reproductive system. *Int. J. Mol. Sci.* **19**, 1842.

Ho TY, Wu SL, Chen JC, Li CC and Hsiang CY. Emodin blocks the SARS coronavirus spike protein and angiotensin-converting enzyme 2 interaction. Antiviral research, 2007, 74(2), 92–101.

Hoever G, Baltina L, Michaelis M, Kondratenko R, Baltina L, Tolstikov GA, Doerr HW and Cinatl J. Antiviral activity of glycyrrhizic acid derivatives against SARS-coronavirus. Journal of medicinal chemistry, 2005, 48(4), 1256–1259.

Hoffmann M, Kleine-Weber H, Schroeder S, Krüger N, Herrler T and Erichsen S. SARS-CoV-2 cell entry depends on ACE2 and TMPRSS2 and is blocked by a clinically proven protease inhibitor. Cell, 2020, 181, 271–280.

Ibrahim IM, Abdelmalek DH, Elshahat ME and Elfiky AA. COVID-19 spike-host cell receptor GRP78 binding site prediction. J. Infect. 2020, 80, 554–562.

Jeon SR, Kang JW, Ang L, Lee HW, Lee MS, Kim TH. Complementary and alternative medicine (CAM) interventions for COVID-19: An overview of systematic reviews. Integr Med Res. 2022 Sep;11(3):100842. doi: 10.1016/j.imr.2022.100842.

Kadowaki H. and Nishitoh H. 2013 Signaling pathways from the endoplasmic reticulum and their roles in disease. *Genes (basel).* **4**, 306–333.

Khanal P, Dey YN, Patil R, Chikhale R, Wanjari MM, Gurav SS, Patil BM, Srivastava B, Gaidhani SN. Combination of system biology to probe the anti-viral activity of andrographolide and its derivative against COVID-19. RSC Adv. 2021 Jan 27;11(9):5065-5079. doi: 10.1039/d0ra10529e. PMID: 35424441; PMCID: PMC8694486.

Krijnse-Locker J, Ericsson M, Rottier PJM and Griffiths G. Characterization of the budding compartment of mouse hepatitis virus: evidence that transport from the RER to the golgi complex requires only one vesicular transport step, J. Cell Biol., 1994, 124, 55-70, 10.1083/jcb.124.1.55

Kumar G, Kumar D, Singh NP. Therapeutic Approach against 2019-nCoV by Inhibition of ACE-2 Receptor. Drug Res (Stuttg). 2021 Apr;71(4):213-218. doi: 10.1055/a-1275-0228. Epub 2020 Nov 12. PMID: 33184809; PMCID: PMC8043666.

Li W. Angiotensin-converting enzyme 2 is a functional receptor for the SARS coronavirus. Nature 426, 450–454 (2003).

Lin C.W., Tsai F.J., Tsai C.H., Lai C.C., Wan L., Ho T.Y. Anti-SARS coronavirus 3C-like protease effects of *Isatisindigotica* root and plant-derived phenolic compounds. *Antivir. Res.* 2005;68:36–42.

Lipinski CA (2004) Lead-and drug-like compounds: the rule-of-five revolution. Drug Discov Today Technol 1:337–341.

Mollica V, Rizzo A, Massari F. The pivotal role of TMPRSS2 in coronavirus disease 2019 and prostate cancer. Future Oncol. 2020; 16(27):1-5. https://doi.org/10.2217/fon-2020-0571; Strope JD, PharmD CHC, Figg WD. TMPRSS2: potential biomarker for COVID-19 outcomes. J Clin Pharmacol. 2020;60(7):801-807. https://doi.org/10.1002/jcph.1641.

Morris G. M., Huey R., Lindstrom W., Sanner M. F., Belew R. K., Goodsell D. S. and Olson A. J. 2009 Autodock4 and AutoDockTools4: automated docking with selective receptor flexibility. *J. Comput. Chem.* **16**, 2785–2791.

Muralidar S, Ambi SV, Sekaran S, Krishnan UM. The emergence of COVID -19 as a global pandemic: understanding the epidemiology, immune response and potential therapeutic targets of SARS -CoV - 2. Biochimie. 2020;179:85 -100. https://doi.org/10.1016/j.biochi. 2020.09.018.

Ni M, Zhang Y, Lee AS. Beyond the endoplasmic reticulum: atypical GRP78 in cell viability, signalling and therapeutic targeting. Biochem J. 2011;434:181-188.

Orhan IE, andSenolDeniz FS. Natural Products as Potential Leads Against Coronaviruses: Could They be Encouraging Structural Models Against SARS-CoV-2?. Nat. Prod. Bioprospect., 2020, 10, 171–186.

Poduri R, Joshi G, Jagadeesh G. Drugs targeting various stages of the SARS-CoV-2 life cycle: exploring promising drugs for the treatment of Covid-19. Cell Signal. 2020;74(July):109721. https:// doi.org/10.1016/j.cellsig.2020.109721.

Rasool MS, Siddiqui F, Hassan MA, Hafiz S. Novel Coronavirus-2019 (2019-nCoV): Perspectives of emergence, prophylaxis and predicted treatment approaches. Pak J Pharm Sci. 2020 Sep;33(5):2199-2207. PMID: 33824130.

Shen J., Chen X., Hendershot L., Prywes R. ER stress regulation of ATF6 localization by dissociation of BIP/GRP78 binding and unmasking of Golgi localization signals. *Dev. Cell.* 2002;3(1):99–111.

Shin J, Toyoda S, Fukuhara A, Shimomura I. GRP78, a Novel Host Factor for SARS-CoV-2: The Emerging Roles in COVID-19 Related to Metabolic Risk Factors. Biomedicines. 2022 Aug 17;10(8):1995. doi: 10.3390/biomedicines10081995.

Shin J, Toyoda S, Nishitani S, Fukuhara A, Kita S, Otsuki M, Shimomura I. Possible Involvement of Adipose Tissue in Patients With Older Age, Obesity, and Diabetes With SARS-CoV-2 Infection (COVID-19) via GRP78 (BIP/HSPA5): Significance of Hyperinsulinemia Management in COVID-19. Diabetes. 2021 Dec;70(12):2745-2755. doi: 10.2337/db20-1094.

Sridhar S, Saha G, Lata S and Mehrotra R. Molecular docking studies of Indian variants of pathophysiological proteins of SARS-CoV-2 with selected drug candidates. J Genet, 2021, 100(2), 64. doi: 10.1007/s12041-021-01313-2. PMID: 34553696; PMCID: PMC8435403.

Srikanth, L., Sarma, P.V.G.K. Andrographolide binds to spike glycoprotein and RNA-dependent RNA polymerase (NSP12) of SARS-CoV-2 by in silico approach: a probable molecule in the development of anti-coronaviral drug. *J Genet EngBiotechnol* **19**, 101 (2021). https://doi.org/10.1186/s43141-021-00201-7

To KK, Tsang OT and Leung WS. Temporal profiles of viral load in posterior oropharyngeal saliva samples and serum antibody responses during infection by SARS-CoV-2: an observational cohort study, Lancet Infect. Dis., 2020, 20, 565-574, 10.1016/S1473-3099(20)30196-1

Trott O, Olson AJ. AutoDock Vina: improving the speed and accuracy of docking with a new scoring function, efficient optimization, and multithreading. J ComputChem. 2010 Jan 30;31(2):455-61. doi: 10.1002/jcc.21334. PMID: 19499576; PMCID: PMC3041641.

ulQamar T, Alqahtani SM, Alamri MA and Chen LL. Structural basis of SARS-CoV-2 3CLpro and anti-COVID-19 drug discovery from medicinal plants, J. Pharm. Anal., 2020, 10, 313-319, 10.1016/j.jpha.2020.03.009

van Dijk AD, de Vries SJ, Dominguez C, Chen H, Zhou HX, Bonvin AM. Data-driven docking: HADDOCK's adventures in CAPRI. Proteins. 2005 Aug 1;60(2):232-8. doi: 10.1002/prot.20563. PMID: 15981252.

Veerasamy R, Karunakaran R. Molecular docking unveils the potential of andrographolide derivatives against COVID-19: an in silico approach. J Genet EngBiotechnol. 2022 Apr 14;20(1):58. doi: 10.1186/s43141-022-00339-y. PMID: 35420322; PMCID: PMC9008396.

Wang M, Wey S, Zhang Y, Ye R and Lee AS. Role of the unfolded protein response regulator GRP78/BiP in development, cancer, and neurological disorders. Antioxid Redox Signal, 2009, 11, 2307–2316.

Wang W., Xu Y., Gao R., Lu R., Han K., Wu G. and Tan W. 2020b Detection of SARS-CoV-2 in different types of clinical specimens. *JAMA.* **323**, 1843–1844.

Wang X, Xia S, Wang Q. Broad-spectrum coronavirus fusion inhibitors to combat COVID-19 and other emerging coronavirus diseases. Int J Mol Sci. 2020;21(11):3843. https://doi.org/10.3390/ ijms21113843

Xian Y, Zhang J, Bian Z, Zhou H, Zhang Z, Lin Z and Xu H. Bioactive natural compounds against human coronaviruses: a review and perspective. Acta. Pharmaceut. Sinica-B, 2020, 10(7), 1163–1174. https://doi.org/10.1016/ j.apsb.2020.06.002.

Xiang, Y. F., Ju, H. Q., Li, S., Zhang, Y. J., Yang, C. R., & Wang, Y. F. (2010). Effects of 1,2,4,6-tetra-O-galloyl-β-D-glucose from *P. emblica* on HBsAg and HBeAg secretion in HepG 2.2.15 cell culture. VirologicaSinica, 25(5), 375–380.

Yang P and Wang X. COVID-19: a new challenge for human beings. Cell. Mol. Immunol., 2020, 17, 555–557.

Ziebuhr J, Snijder EJ and Gorbalenya AE. Virus-encoded proteinases and proteolytic processing in the Nidovirales, J. Virol., 2000, 81 (4), 853-879, 10.1099/0022-1317-81-4-853.